

Highly Selective Macrocyclic Formations by Metathesis Catalysts Fixated in Nanopores

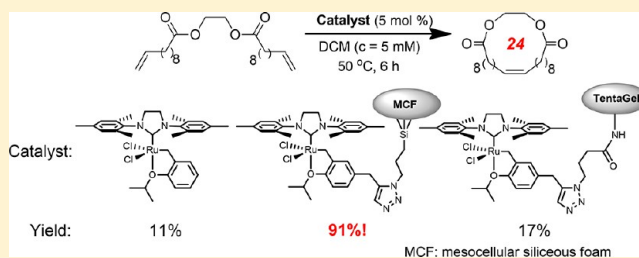
Joo-Eun Jee,[†] Jian Liang Cheong,[†] Jaehong Lim,[†] Cheng Chen,[‡] Soon Hyeok Hong,^{*,‡} and Su Seong Lee^{*,†}

[†]Institute of Bioengineering and Nanotechnology, 31 Biopolis Way, The Nanos, Singapore 138669

[‡]Center for Nanoparticle Research, Institute for Basic Science, and Department of Chemistry, College of Natural Sciences, Seoul National University, Seoul 151-747, Korea

S Supporting Information

ABSTRACT: Ruthenium-based metathesis catalysts immobilized on mesocellular siliceous foam (MCF) bearing large nanopores proved highly efficient and selective for macrocyclic ring-closing metathesis (RCM). Kinetic studies revealed that the homogeneous counterpart exhibited far higher activity that accounted for more oligomerization pathways and resulted in less macrocyclization products. Meanwhile, the immobilized catalysts showed lower conversion rates leading to higher yields of macrocyclic products in a given reaction time, with conversion rates and yields dependent upon pore size, catalyst loading density, and linker length. The macrocycle formations via RCM were accelerated by increasing the pore size and decreasing the catalyst loading density while retaining the comparably high yield. The catalysts immobilized on MCF, of which silica surface is rigid and pores are relatively large, showed high conversion rates and yields compared with an analogue immobilized on TentaGel resins, of which backbone becomes flexible upon swelling in the reaction medium. It is noteworthy that the selectivity for the macrocyclic RCM can be significantly improved by tuning the catalyst initiation rates via immobilization onto the support materials in which well-defined three-dimensional network of large nanopores are deployed.



INTRODUCTION

Ring-closing metathesis (RCM) has become one of the standard methods for the synthesis of cyclic compounds largely due to the development of highly active, functional group tolerant, and easily handled catalysts.¹ However, one of the unsolved problems to utilize RCM in the synthesis of medium to large cyclic compounds, important targets in natural product synthesis and pharmaceutical industry, is the limited selectivity caused by equilibrium between intramolecular ring-closing and intermolecular oligomerization.² A conventional way to circumvent the intermolecular pathways is to adopt high-dilution conditions, which is not practical and environmentally benign. Besides, higher catalyst loadings are often required especially for the macrocyclization under high-dilution conditions due to limited catalyst lifetime and efficiency.^{1–3} Grubbs, Stoddart, and co-workers reported template-directed RCM approaches for the selective macrocycle formation of certain olefinic polyethers using secondary dialkylammonium ions as the template.⁴ However, the template-directed RCM methods, working on the specifically functionalized substrates, cannot serve as an ideal solution for the synthesis of various kinds of macrocycles. Therefore, it is highly desirable to develop efficient olefin metathesis catalysts that are selective for macrocyclization in particular.

To address this challenge, we investigated the efficiency of ruthenium-based olefin metathesis catalysts covalently immo-

bilized on mesoporous silica materials with uniform nanopores for macrocyclic RCM. Hoveyda–Grubbs-type derivatives were chosen due to the robust nature, which can be immobilized via several ways such as fluorinated carboxylates,⁵ benzylidene,⁶ and N-heterocyclic carbene (NHC).⁷ Although the immobilization via functionalized NHC ligands was expected to give permanently anchored catalysts due to strong coordination of NHC to ruthenium, these catalysts have often suffered from low immobilization efficiency as well as decreased yield during sequential runs. A majority of such supported catalysts have been easily prepared via modified 2-isopropoxystyrenyl ligand although the catalytic reactions of these supported catalysts do not proceed in an authentic heterogeneous fashion.⁸ However, these immobilized catalysts demonstrated good reusability, presumably due to incomplete activation of the immobilized precatalysts, as suggested by Plenio and co-workers.⁸ Although several groups reported the use of metathesis catalysts immobilized on porous silica or polymer supports, they mostly focused on reusability of the catalysts for making relatively small- to medium-sized rings.⁹

The recently developed ruthenium-based olefin metathesis catalysts supported on mesocellular siliceous foams (MCF) were demonstrated as a good tool for the RCM of relatively

Received: January 9, 2013

Published: February 22, 2013

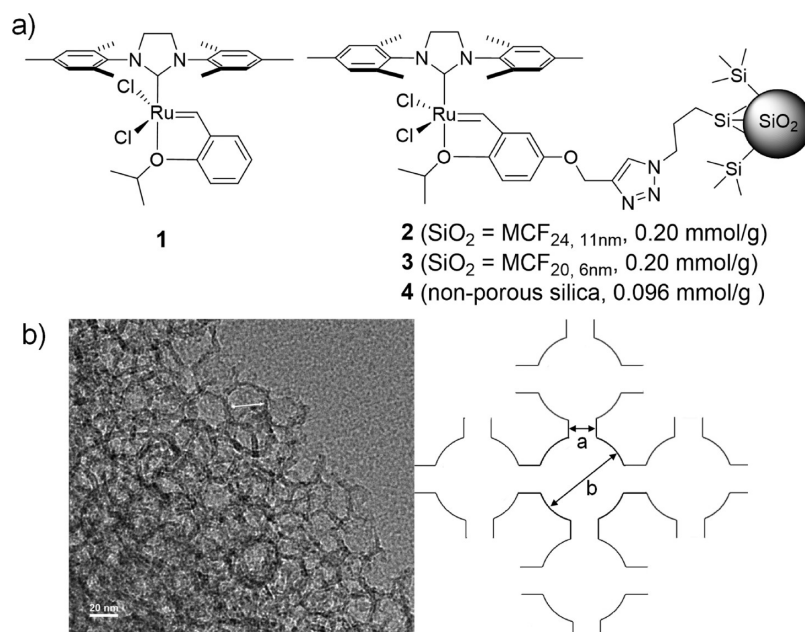


Figure 1. (a) Ruthenium-based olefin metathesis catalysts investigated. (b) TEM image of the catalyst 3 and schematic diagram of MCF (a: window pore, b: cell pore).

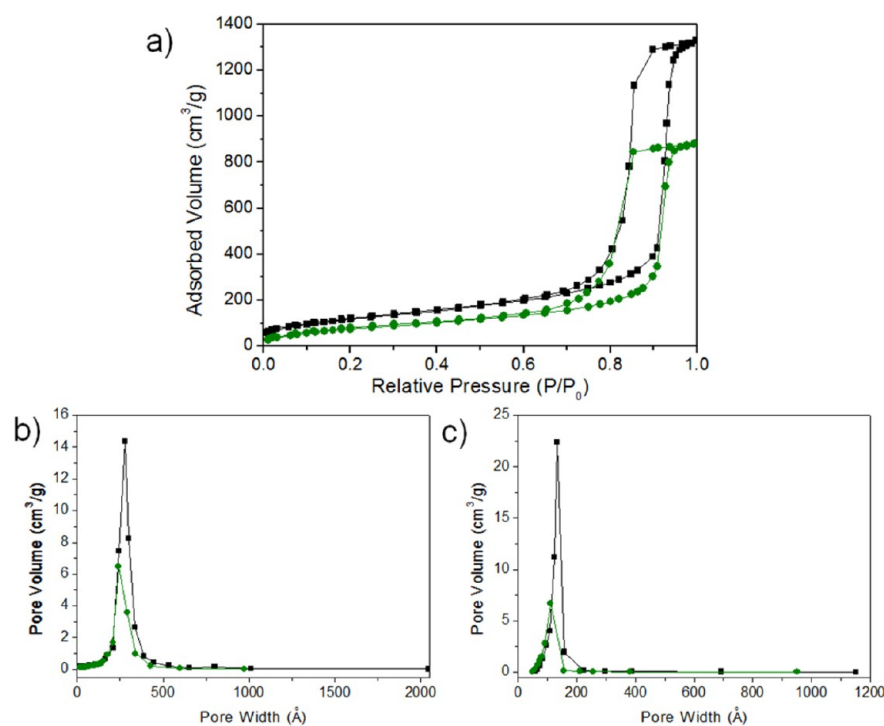


Figure 2. (a) Nitrogen adsorption–desorption isotherms, (b) cell pore distributions, and (c) window pore distributions of MCF for the bare support (■) and the catalyst 2 (●).

small diene substrates.¹⁰ The spherical microparticles of MCF can be considered as a complex of 3-dimensionally interconnected nanoreactors with catalysts immobilized on the reactor wall. Mesoporous silica materials have been used for immobilization of various catalysts due to their high surface area and uniform pores.¹¹ In particular, its relatively large pores can facilitate the diffusion of relatively large substrates. Typically, more than 95% of the surface areas come from the inner pores. Once the catalysts are immobilized on the inner surface, most of them are isolated from the bulk environments

accommodating the reactions in nanopores. In some cases, it has been observed that catalysts showed unexpected phenomena upon immobilization in such a confined space.¹²

Although the reactive catalytic species might be released into reaction medium in catalytic cycles, we envisioned that the intriguing nature of the nanoporous silica supports would bias the selectivity between macrocyclization and oligomerization, presumably due to the differences in kinetic behaviors of the catalysts both upon initiation and substrate diffusion. Herein, we prepared a series of MCF-supported metathesis catalysts to

investigate the effects of pore size, catalyst loading density and linker length for immobilization of the aryl ligand on macrocyclic RCM. These studies will facilitate the development of catalytic systems that are kinetically optimized for macrocyclic RCM.

RESULTS AND DISCUSSION

Synthesis of Ruthenium-Based Metathesis Catalysts Supported on MCF. The silica-based support material was synthesized by the reported procedure.¹³ MCF is a mesoporous silica material with uniformly large nanopores (>7 nm) and high surface areas (>400 m²/g). It has two types of pores: cell pores and window pores. Cell pores are fully connected one another through window pores leading to a 3-dimensional interconnected pore structure, which facilitate mass transfer and molecular diffusion (Figure 1b). The pore size of MCF could be further controlled by adjusting aging temperature and adding ammonium fluoride prior to aging at high temperature.

The MCF-supported metathesis catalysts (**2** and **3**) were synthesized by the reported procedure (Figure 1, MCF_{cell, window}), which included the modification of 2-isopropoxystyrenyl ligand via click chemistry for covalent attachment to silica wall surface of MCF.^{10b} The cell pore sizes of MCF decreased upon immobilization, which confirmed the inner pore functionalization (Figure 2 and Table 1). Cross-

Table 1. Characterization^a of the Support Materials and the Catalysts

material	surface area (m ² /g)	cell pore size (nm)	window pore size (nm)
MCF for 2	431	28.0	13.5
catalyst 2	292	23.9	11.3
MCF for 3	613	22.3	7.5
catalyst 3	334	20.4	6.3

^aDetermined from N₂ sorption isotherms. The pore sizes were calculated from the adsorption branches based on the BdB sphere model. The window sizes were calculated from the desorption branches based on the BdB sphere model.

polarization magic angle spinning (CPMAS) ¹³C and ²⁹Si NMR spectra of the catalysts confirmed the immobilization of NHC-ruthenium catalysts on the silica surface of MCF (see the Supporting Information, Figure S7). These immobilized catalysts displayed green color that is typical for the homogeneous Hoveyda–Grubbs catalysts. The TEM image and EDS analysis of the catalyst **2** exhibit uniform distribution of the ruthenium complexes through the whole surface of MCF (see the Supporting Information, Figure S6). In the previous works, the catalyst **2** showed excellent reactivity and reusability in the formation of 5-, 6-, and 7-membered cyclic compounds.¹⁰ The catalyst **3** was synthesized to investigate the effects of pore size in macrocyclic RCM.

Macrocyclic RCM Reactions. Initially, the MCF-supported catalysts (**2** and **3**) were tested for macrocyclic RCM reactions with a series of large substrates that have been rarely tested with immobilized metathesis catalysts to date (Table 2). The results were compared with the analogous homogeneous catalyst (**1**). To our delight, the immobilized catalysts **2** and **3** gave superior yields to the homogeneous counterpart (**1**) for all kinds of large substrates tested (Table 2). The selectivity difference between **1** and **2** (or **3**) became more noticeable when the ring sizes increased (entries 3–12). For greater than 24-membered rings,

Table 2. Macrocyclic RCM by 1-4

Entry	RCM product	Ring size	Catalyst	Time (hr)	Yield (%) ^a	E/Z ^b
1		14	1	6	74	10.0
			2	6	83	13.0
			3	6	79	11.7
			4	6	61	11.2
2		16	1	5	53	3.6
			2	5	96	3.3
			3	5	89	3.3
			4	5	77	3.5
3		20	1	6	29	2.1
			2	6	62	2.3
			3	6	55	2.4
			4	6	28	2.6
4		21	1	8	19	2.2
			2	8	68	2.3
			3	8	62	2.3
			4	8	48	2.3
5		21	1	6	9	2.0
			2	6	35	2.1
			3	6	30	2.1
			4	8	25	2.2
6		21	1	6	10	1.9
			2	6	35	2.1
			3	6	30	2.2
			4	6	26	2.2
7		24	1	6	11	2.8
			2	6	91	2.9
			3	6	86	3.1
			4	6	45	3.1
8		24	1	6	9	2.1
			2	6	91	2.4
			3	6	90	2.4
			4	6	38	2.4
9		24	1	9	6	2.5
			2	9	75	2.6
			3	9	71	2.6
			4	9	28	2.8
10		25	1	6	19	2.2
			2	6	71	2.7
			3	6	70	2.6
			4	6	42	2.5
11		26	1	6.5	18	2.5 ^c
			2	6.5	70	3.4 ^c
			3	6.5	68	3.4 ^c
			4	6.5	36	3.3 ^c
12		27	1	7	9	2.1
			2	7	58	3.1
			3	7	58	2.9
			4	7	28	2.8

^aDetermined by GC using *n*-dodecane as an internal standard, average of at least two runs. ^bDetermined by GC (Supporting Information, Figure S9). ^c1,4-Benzoquinone was used as an additive to prevent the olefin isomerization.

2 and **3** exhibited much higher yields than catalyst **1** demonstrating their exceptional selectivity for macrocyclization (entries 7–12). In the cases of a diene **5k**, olefin isomerization of the cyclized product **6k** were observed by ¹³C NMR spectroscopy, which was reported as a major side reaction in olefin metathesis due to catalyst decomposition.¹⁴ The reported method using 1,4-benzoquinone was effective to suppress the isomerization without significantly reducing the yields of **6k** (entry 11).^{14a} The catalyst **3** produced slightly lower yields than the catalyst **2**, which accounts for a negligible effect of pore size within the tested reaction time.

Design of Various Supported Ruthenium-Based Olefin Metathesis Catalysts. Motivated by the unexpectedly high selectivity of the MCF-supported catalysts in macrocyclic RCM, we examined various factors that might affect the

catalytic selectivity. The factors include catalyst loading density, linker length, pore size, and the type of support materials. These are illustrated schematically in Figure 3.

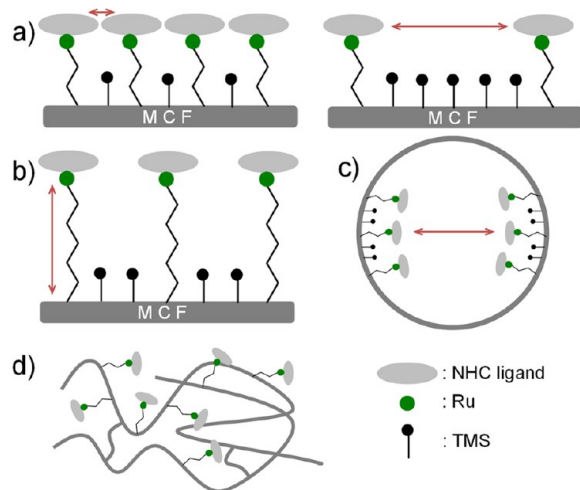


Figure 3. Schematic views of (a) loading density, (b) linker length, and (c) pore size to control in MCF-supported catalysts and (d) polymer-supported analogue.

Based on these factors, various types of catalysts were prepared including MCF-supported catalysts (7–10) with different catalyst loading or linker length as well as nonporous silica-supported (4) and TentaGel-supported (11) derivatives (Figures 1 and 4). The precapping method¹⁶ was used for

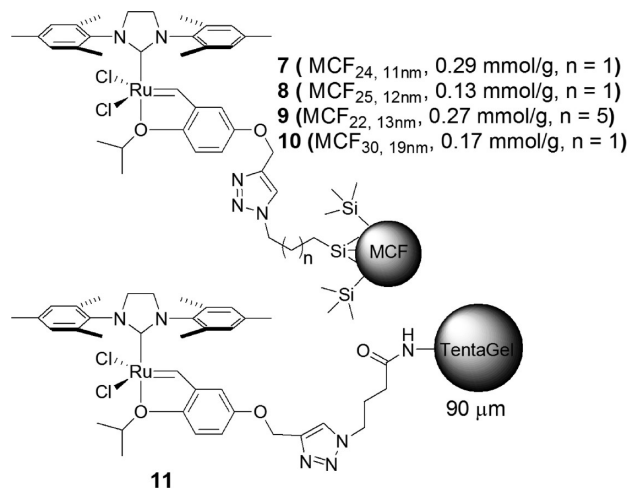


Figure 4. More ruthenium-based olefin metathesis catalysts investigated.

uniform distribution of catalysts on the surface of MCF. TentaGel resin is a grafted copolymer consisting of polyethylene glycol attached to low cross-linked polystyrene matrix through ethereal linkage. The amphiphilic polymer displays excellent swelling capacity in dichloromethane as a reaction medium for RCM.¹⁷ Therefore, it serves as a suitable polymer support for comparison with MCF. The cell pore sizes of MCF decreased upon immobilization, which confirmed the inner pore functionalization (Table 3 and Figures S2–S5, Supporting Information). Solid-state CPMAS ¹³C and ²⁹Si NMR confirmed

the immobilization of Hoveyda–Grubbs-type catalysts (Supporting Information, Figure S7).

Table 3. Characterization^a of the Support Materials and the Catalysts

material	surface area (m ² /g)	cell pore size (nm)	window pore size (nm)
MCF for 7–9	431	28.0	13.5
catalyst 7	257	23.5	10.5
catalyst 8	285	24.8	12.3
catalyst 9	324	22.1	12.8
MCF for 10	286	38.9	23.1
catalyst 10	247	30.4	19

^aDetermined from N₂ sorption isotherms. The pore sizes were calculated from the adsorption branches based on the BdB sphere model. The window sizes were calculated from the desorption branches based on the BdB sphere model.

A ruthenium-based catalyst supported in nonporous submicro-sized silica (4) was prepared in order to study the effects of the nanopores on the improved selectivity toward RCM over intermolecular reactions. To synthesize small silica particles with high surface area, an aqueous ethanol solution was oversaturated with NH₃ prior to the addition of tetraethyl orthosilicate (TEOS), which resulted in the formation of 100–200 nm nonporous silica particles. The aryl ligand was immobilized on the surface of the silica particles without complete drying to avoid the aggregation of the silica particles, which can generate interparticle pores. Figure 5 shows completely separated silica particles after the catalyst immobilization. Solid-state CPMAS ¹³C and ²⁹Si NMR confirmed the immobilization of Hoveyda–Grubbs-type catalysts on the silica surface (Supporting Information, Figure S7). Catalyst 4 consistently exhibited lower activity and lower product yield than the MCF-supported catalysts 2 and 3 in the tested reactions (Table 2). The considerably lower surface area of the nonporous silica led to extremely high density of catalysts loaded on the limited silica surface. These encumbering environments might result in difficult access of large substrates to the metal catalytic centers, which are surrounded by the bulky NHC ligand and silica surface via covalent linkage. However, the yields of macrocyclic products by 4 were still higher than those by the homogeneous catalyst (1) at the given reaction time. These results imply that the immobilization of the homogeneous catalyst on a silica surface may be one successful factor to improve the selectivity in macrocyclic RCM, presumably due to slow initiation of catalytic cycle.

Kinetic Studies. For better comparison among the homogeneous (1) and the heterogeneous catalysts (2, 3, and 7–11), progress of both the formation of a RCM product (6g) and the consumption of a substrate (5g) were monitored. The homogeneous catalyst 1 completed consumption of the starting material 5g within 15 min and produced equilibrium mixtures of 6g and cross-metathesis products (oligomeric compounds) as time elapsed.^{2d} However, all the MCF-supported catalysts showed slower consumption of 5g and much higher yield of 6g (Figure 6). Through the localization of catalysts on porous support materials, large substrate might take less chance to encounter the reactive catalyst than in a homogeneous reaction. In addition, the ratio of substrate to catalyst in nanopores is much lower than that in the bulky solution of the homogeneous

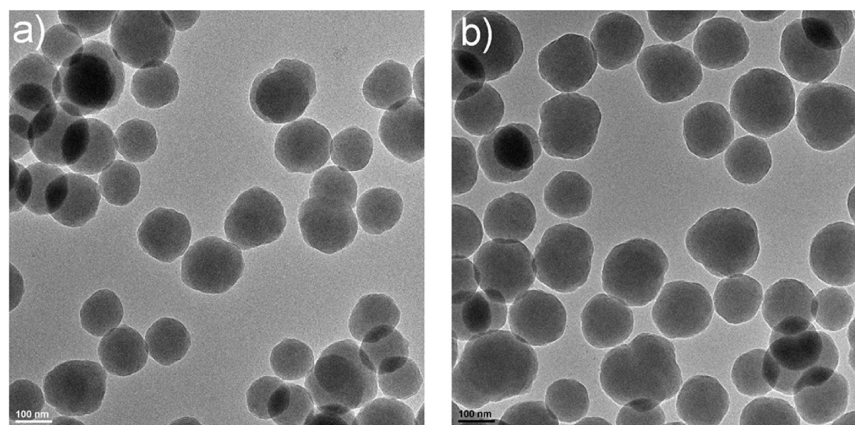


Figure 5. TEM images of nonporous catalyst (4) (a) before and (b) after immobilization.

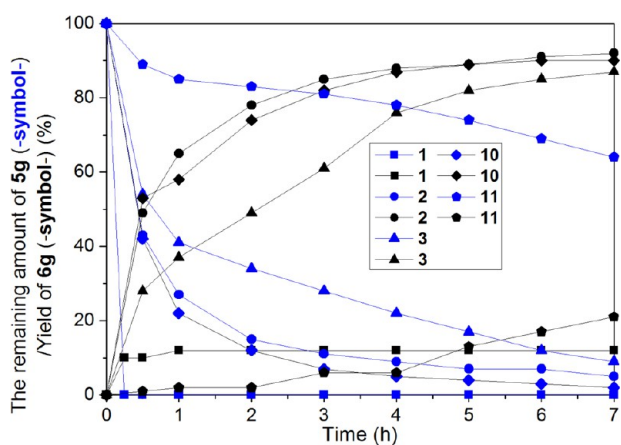


Figure 6. Consumption of **5g** (blue symbols) and formation of **6g** (black symbols) by metathesis catalysts. The conversion of **5g** (%) = 100% – the remaining amount of **5g** (%).

reaction. This might account for higher yield of macrocycles in the RCM reactions by the MCF-supported catalysts. The extremely fast initial activation of the homogeneous catalyst may make the reactions proceed less selectively to result in dominant formation of oligomers as undesired products.

Figure 6 also indicates that the conversion rate of **5g** depends on the pore size of MCF and the type of support materials. When the window pore size of MCF increased from 6 (catalyst 3) to 16 nm (catalyst 10), **5g** was more converted, e.g., in 1 h, from 59 to 79% due to the facilitated diffusion of the large substrate. All the MCF-supported catalysts showed excellent yields of **6g** at a reaction time of 6 h. TentaGel-supported catalyst (11) showed sluggish consumption of **5g** combined with slow increase of **6g** presumably due to the restricted diffusion of the large substrate (**5g**) into catalysts embedded in polymer matrix. The catalyst 11 achieved only 31% conversion at 6 h of reaction time compared with 93% conversion by 2 due to inefficient diffusion of the large substrate into the polymer matrix with highly flexible structure. However, the yield of **6g** by the catalyst 11 continued to increase upon time. These results also support our hypothesis that the slow catalyst activation should be one important factor to improve the yield in macrocyclic RCM. In addition, this clearly demonstrates the benefits of the rigid mesoporous silica support with large nanopores in the diffusion of large substrates.

Figure 7 shows the effect of catalyst loading density and linker length on macrocyclic RCM. When the catalyst loading

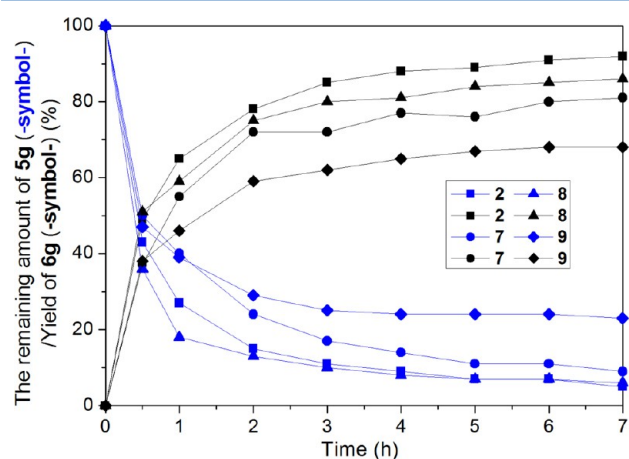


Figure 7. Consumption of **5g** (blue symbols) and formation of **6g** (black symbols) by metathesis catalysts. The conversion of **5g** (%) = 100% – the remaining amount of **5g** (%).

on MCF was increased from 0.13 (catalyst 8) to 0.28 mmol/g (catalyst 7), the conversion of **5g** was decreased from 82 to 60% at 1 h. The metal catalytic center (Ru) is sandwiched between the bulky NHC ligand and silica wall as depicted in Figure 3. Therefore, the higher catalyst loading might lead to the increase of steric hindrance surrounding the ruthenium catalytic center. Sequentially, it is getting more difficult for the large substrate to access the ruthenium, which might result in the decrease of conversion rate. These results also elucidate that the low conversion rate of nonporous silica-supported catalyst (4) may be caused by highly encumbered environments surrounding the metal catalytic center originated from the relatively high catalyst loading density on limited silica surface compared to mesoporous silica with extremely high surface area. The high catalyst loading density on the silica surface was confirmed by the low amount of TMS postcapping, compared with the MCF-supported catalysts, in the solid-state NMR of the catalyst 4.

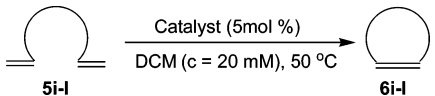
Initially, the increase of linker length was expected to enhance the activity of the MCF-supported catalyst with high catalyst loading due to easier access of substrates to the metal centers. However, the increase of linker length at high loading (catalyst 9) turned out distracting the conversion rate (Figure

7). There was nearly no catalytic activity after 3 h possibly due to fast deactivation of the immobilized catalysts through a decomposition pathway via the formation of bimetallic species,^{3,18} which might be caused by facile intermolecular perturbations, or faster catalyst initiation followed by decomposition between the catalysts through the long flexible linker. Consequently, it led to the decrease of the yield, which clearly correlates with our previous results.^{5a}

Based upon these results, the catalytic systems for macrocyclic RCM can be optimized through well-designed immobilization of homogeneous metathesis catalysts on mesoporous silica materials with relatively large nanopores. MCF is proven to be one of excellent support materials for it due to facile control of pore size and fully interconnected pore structure.

Macrocyclic RCM Reactions at Higher Concentrations. Encouraged by these results, RCM reactions for 24- to 27-membered ring synthesis were conducted at an increased substrate concentration of 20 mM (Table 4). The immobilized

Table 4. Macrocyclic RCM by 1–3 under Higher Substrate Concentration



entry	product	ring size	catalyst	time (h)	yield ^a (%)	E/Z ^b
1	6i	24	1	5	5	2.5
			2	5	50	2.6
			3	5	43	2.6
2	6j	25	1	5	5	2.2
			2	5	52	2.7
			3	5	50	2.6
3	6k	26	1	4	7	2.5 ^c
			2	4	55	3.4 ^c
			3	4	46	3.4 ^c
4	6l	27	1	5	4	3.0
			2	5	42	2.1
			3	5	41	3.1

^aDetermined by GC using *n*-dodecane as an internal standard, average of at least two runs. ^bDetermined by GC (Supporting Information, Figure S10).¹⁵ ^c1,4-Benzoquinone was used as an additive to prevent the olefin isomerization.

catalysts 2 and 3 still exhibited higher activity than the homogeneous analogue 1 with approximately 10-fold increase in yield for macrocycle formations. It is demonstrated that the advantage of the immobilized system was further enhanced at higher concentration of substrates. However, the overall decrease in RCM selectivity was observed in the higher concentration even with 2 and 3, as the competing cross-metathesis reactions were favored, along with the accelerated

initiation of the supported catalysts (entries 9–12 in Table 2 vs Table 4).

CONCLUSION

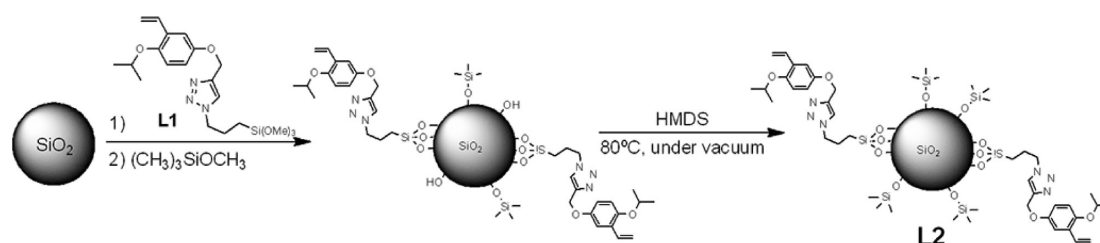
Ruthenium-based metathesis catalysts supported on MCF showed high efficiency in macrocyclic RCM reactions. The immobilized catalysts surpassed the second-generation Hoveyda–Grubbs metathesis catalyst in selectivity especially for the formation of greater than 20-membered rings. The kinetic studies implied that the sluggish activation of the supported catalysts led to high selectivity for macrocyclic products. In the corresponding homogeneous system, the extremely fast activation of the catalysts resulted in low yields due to high occurrence of competing pathways to oligomerization via cross-metathesis. Yields and conversion rates of MCF-supported catalysts could be improved by adjusting the support pore size and the catalyst loading density. It was also demonstrated that the silica with rigid porous structure was beneficial over a polymer support that highly swells in reaction medium toward facilitating the diffusion of large substrates through the support matrix. In addition, the MCF-supported catalyst showed good reusability in macrocyclic RCM. It is noteworthy that the control of catalyst activity through the immobilization of homogeneous catalysts on mesoporous materials with high surface area can improve the selectivity of catalytic reactions. This result paves a way to the improvement of macrocyclic RCM, potentially applicable in manufacturing.

EXPERIMENTAL SECTION

General Remarks. All reactions were carried out in oven-dried glassware under an inert atmosphere of dry argon. TentaGel S NH₂ resin (capacity: 0.32 mmol/g, diameter: 90 μm) was used as a polymer support. Analytical TLC was performed on a silica gel plate of 0.25 mm in thickness. NMR data were obtained at 298 K at 400 MHz for proton, and at 100 MHz for carbon, respectively, in the indicated solvent and are listed in parts per million downfield from tetramethylsilane (TMS). For MAS experiments, samples were packed into 4 mm ZrO₂ rotors and spun at 10 kHz. Spectra were calibrated against an external standard of adamantane. To recognize spinning sidebands, a second spectrum was recorded at a spinning rate of 8 kHz, so that spinning sidebands appeared with different shifts. Mass spectrometry was performed by Q-TOF using Electro Spray Ionization (ESI) mode. Characterization of substrates and isolated RCM products reported are in agreement with the literature reports.

2-Isopropoxystyrenyl Ligand Supported on Nonporous Silica (L2). To a 500 mL conical flask with saturated ammonia solution in ethanol (240 mL) were added aqueous ammonia solution (13 mL, 25 wt %) and tetraethoxy orthosilicate (TEOS, 20 mL) and the mixture stirred overnight. The solution turned milky to give silica nanoparticles. 2-Isopropoxystyrenyl triazole ligand (L1)^{10b} was immobilized directly on the silica particles without isolation of the silica particles. L1 was dissolved in 20 mL of THF and added dropwise at a rate of 5 mL/h to the solution containing silica nanoparticles. Trimethylmethoxysilane (0.5 mL) was subsequently added and the

Scheme 1. Immobilization of the Modified 2-Isopropoxystyrenyl Ligand on Nonporous Silica



mixture stirred for 2 h. The resulting solution was centrifuged for 45 min at 4800 rpm and washed with methanol and DCM. The synthesized nonporous silica was dried overnight at 80 °C. Postcapping of the silica was carried out by injecting hexamethyldisilazane (HMDS, 1 mL) and kept under reduced pressure at 80 °C for 6 h. The resulting solid was cooled to ambient temperature, washed with methanol and DCM, and dried under reduced pressure to yield nonporous silica-supported 2-isopropoxystyrenyl ligand (L2) as a white powder (Scheme 1). Anal. Calcd: C, 1.73; H, 1.27; N, 0.36.

Ruthenium-Based Metathesis Catalyst Supported on Nonporous Silica (4). L2 (1.55 g) was dried overnight under reduced pressure at 80 °C. The reaction vessel was allowed to cool to ambient temperature, prior to the addition of **1** (140 mg, 0.165 mmol) and CuI (16.3 mg, 0.165 mmol) in a glovebox. DCM (15 mL) was subsequently added, and the resultant mixture was allowed to reflux at 50 °C for 5 h under argon atmosphere. The reaction mixture was centrifuged for 45 min at 4800 rpm, and then the supernatant was discarded. Subsequent washings were carried out several times with anhydrous DCM and anhydrous methanol until the supernatant became a clear colorless solution. All of the supernatant fractions were collected for ICP-MS to measure the loading amount of ruthenium species in the supported catalyst. The thoroughly washed catalyst particles were dried under reduced pressure for 24 h to yield the immobilized catalyst **4** as a fine green powder. Silica particle aggregation was not observed in catalyst **4**. Anal. Calcd: C, 3.04; H, 1.20; N, 0.55. The catalyst loading amount calculated from the total amount of ruthenium in the combined supernatant fractions: 0.096 mmol/g.

Ruthenium-Based Metathesis Catalyst Supported on MCF (2,3 and 7–10). The ruthenium-based compounds **2**, **3**, and **7–10** were synthesized following the literature procedures.^{10b} MCF with ultralarge nanopores for the catalyst **10** was synthesized following the literature procedures.¹³ An azido-functionalized silane ($\text{N}_3(\text{CH}_2)_7\text{SiMe}(\text{OMe})_2$) was synthesized by the reaction of $\text{Br}(\text{CH}_2)_7\text{SiMe}(\text{OMe})_2$ with sodium azide in anhydrous DMF. ¹H NMR (400 MHz, CDCl_3): δ 0.10 (s, 3H), 0.6 (m, 2H), 1.3 (m, 8H), 1.58 (m, 2H), 3.23 (m, 2H), 3.50 (s, 6H). ¹³C NMR (100 MHz, CDCl_3): δ -5.67, 13.18, 22.76, 26.75, 28.95, 28.99, 33.20, 50.31, 51.62. HRMS (ESI): calcd for $\text{C}_{10}\text{H}_{24}\text{N}_3\text{NaO}_2\text{Si}$ 268.1452, found 268.1458 $[\text{M} + \text{H}]^+$. This azido compound was reacted with the acetylene-functionalized 2-isopropoxystyrene in the presence of copper(I) catalyst to give a clicked product. ¹H NMR (400 MHz, CDCl_3): δ 0.09 (s, 3H), 0.60 (m, 2H), 1.29 (m, 14H), 1.88 (m, 2H), 3.49 (s, 6H), 4.31–4.39 (m, 3H), 5.18 (s, 2H), 5.21 (d, 1H, $J = 11.2$ Hz), 5.67 (d, 1H, $J = 17.8$ Hz), 6.82 (s, 2H), 6.98 (dd, 1H, $J = 17.8$ Hz, 11.2 Hz), 7.11 (m, 1H), 7.56 (s, 1H). ¹³C NMR (100 MHz, CDCl_3): δ -5.71, 13.13, 22.33, 22.71, 26.47, 28.75, 30.38, 33.03, 50.27, 50.54, 62.90, 72.27, 112.71, 114.46, 115.08, 116.82, 122.47, 129.43, 131.78, 144.54, 149.96, 152.64. HRMS (ESI): calcd for $\text{C}_{24}\text{H}_{40}\text{N}_3\text{O}_4\text{Si}$ 462.2783, found 462.2799 $[\text{M} + \text{H}]^+$. The clicked product was immobilized on MCF for the catalyst **7**. All of MCF-supported catalysts were analyzed by the Fourier-transform infrared (FTIR) as well as CP-MAS ¹³C and ²⁹Si NMR spectra. The catalyst loading density was calculated from the remaining amount of ruthenium species unreacted with the 2-isopropoxystyrenyl ligand immobilized on MCF, which was measured by ICP-MS. The loading amount was confirmed by weight increase after reaction with second-generation Grubbs catalysts.

Ruthenium-Based Metathesis Catalyst Supported on Tentagel Resins (11). In a 25 mL Alltech tube equipped with a filter were placed Tentagel S NH_2 resins (1.50 g, 0.32 mmol/g), 4-azidobutanoic acid (930 mg, 0.72 mmol), 1-ethyl-3-(3-dimethylaminopropyl)carbodiimide (270 mg, 1.75 mmol), and *N,N*-diisopropylethylamine (DIPEA) (250 mg, 1.43 mmol) as well as DCM (10 mL). The tube was sealed and attached to a 180° shaker for 24 h at room temperature. The resulting resins were washed with DCM (25 mL \times 3) and dried under reduced pressure. Postacetylation was carried out by adding acetic anhydride (51 mg, 0.497 mmol) to a resin solution of DCM (10 mL) in the presence of DIPEA (250 mg, 1.43 mmol) for 18 h at room temperature. Resins were washed with DCM

(25 mL \times 3) and dried under reduced pressure. Kaiser test carried out on a small portion of the resins showed absence of violet coloration. The following steps were performed in a glovebox. To all the resins were suspended in 8 mL of dry THF, were added **L1** (118 mg, 0.545 mmol), DIPEA (0.20 mL, 1.14 mmol) and CuI (10 mg, 0.05 mmol). The Alltech tube was sealed and attached to a 180-degree shaker for 22 h at room temperature. The resulting resins were washed with THF and DCM (25 mL \times 3, each), and then dried under reduced pressure. In a glovebox, the ligand immobilized on resin (0.69 g) was transferred into a 50 mL Schlenk flask. Second-generation Grubbs catalyst (210 mg, 0.247 mmol), CuCl (25 mg, 0.247 mmol), and DCM (10 mL) were added. The reaction was refluxed for 5 h. The resulting resins were washed with DCM, MeOH, and then DCM (25 mL \times 3, each). Dark green solids obtained were dried overnight under reduced pressure. The catalyst loading amount calculated from the total amount of ruthenium unreacted with the 2-isopropoxystyrenyl ligand immobilized on MCF, which was measured by ICP-MS. The loading amount was confirmed by weight increase after reaction with second-generation Grubbs catalysts.

General Procedure for the Synthesis of Substrates (5b to 5d, 5g, 5j, and 5k). A solution of 10-undecenoyl chloride in DCM was slowly added at 0 °C to a stirred solution of the alcohol and pyridine in DCM. After the mixture was continuously stirred for 6 h at room temperature under argon atmosphere, it was diluted with DCM, washed successively with H_2O , saturated aqueous solution of NaHCO_3 , and brine, dried over Na_2SO_4 , filtered, concentrated to dryness, and then purified by flash column chromatography on silica gel to give the desired compound. Characterization data for **5b**,^{2e} **5c**,¹⁹ **5d**,¹⁹ **5g**,²⁰ **5j**,²¹ and **5k**²⁰ substrates were in agreement with literature reports.

5a. This substrate was prepared and purified as explained in the general procedure using 3-buten-1-ol (1.08 g, 15.0 mmol), 10-undecenoyl chloride (2.35 g, 11.6 mmol), and pyridine (2.75 g, 34.8 mmol). Flash column chromatography (hexane/EtOAc = 50:1) furnished **5a** (1.30 g, 47%) as a colorless liquid. ¹H NMR (CDCl_3 , 400 MHz): δ 5.89–5.23 (m, 2H), 5.13–4.91 (m, 4H), 4.14 (t, 2H, $J = 6.4$ Hz), 2.42–2.32 (m, 2H), 2.31 (t, 2H, $J = 7.2$ Hz), 2.00–2.09 (m, 2H), 1.67–1.54 (m, 2H), 1.39–1.25 (m, 10H). ¹³C NMR (CDCl_3 , 100 MHz): δ 173.8, 139.1, 134.0, 117.1, 114.1, 63.2, 34.3, 33.7, 33.1, 29.2, 29.28, 29.20, 29.1, 29.0, 28.8, 24.9. HRMS (ESI): calcd for $\text{C}_{15}\text{H}_{27}\text{O}_2$ 239.2011, found 239.2004 $[\text{M} + \text{H}]^+$.

5e. 10-Undecenoyl chloride (1.48 g, 7.30 mmol) in DCM (10 mL) was added dropwise at 0 °C to a mixture of *p*-toluenesulfonyl amide (0.5 g, 2.92 mmol) and KOH (0.49 g, 8.76 mmol) in dry DCM (30 mL). The resulting mixture was stirred at this temperature for 2 h under N_2 , after which it was allowed to warm to room temperature. After being stirred for another 6 h, the reaction was quenched with H_2O (50 mL), and the aqueous layer was extracted with DCM (30 mL \times 2). The combined organic layers were washed successively with saturated aqueous solution of NaHCO_3 and brine (30 mL each), dried over Na_2SO_4 , filtered, and concentrated to dryness. Flash column chromatography (hexane/EtOAc = 1:1) afforded **5e** (1.80 g, 71%) as a colorless liquid. ¹H NMR (CDCl_3 , 400 MHz): δ 7.91 (d, 2H, $J = 8.24$ Hz), 7.34 (d, 2H, $J = 8.24$ Hz), 5.85–5.75 (m, 2H), 5.02–4.92 (m, 4H), 2.67 (t, 4H, $J = 7.3$ Hz), 2.45 (s, 3H), 2.06–2.00 (m, 4H), 1.64–1.59 (m, 4H), 1.38–1.26 (m, 20H). ¹³C NMR (CDCl_3 , 100 MHz): δ 174.7, 145.8, 139.1, 136.1, 129.8, 128.4, 114.1, 39.3, 33.7, 29.2, 29.1, 29.0, 28.8, 28.6, 24.0, 21.7. HRMS (ESI): calcd for $\text{C}_{29}\text{H}_{46}\text{NO}_4\text{S}$ 504.3148, found 504.3152 $[\text{M} + \text{H}]^+$.

5f. To a solution of NH_3 (1.67 g, 98 mmol) in THF was added 10-undecenoyl chloride (1.00 g, 4.93 mmol). The mixture was stirred for 6 h. The monoacyl amide was isolated by extraction with Et_2O (40 mL \times 3) and purification by quick filtration using flash column chromatography to give a white solid (0.60 g, 80%). To a solution of monoacyl amide (0.57 g, 3.11 mmol) in DCM (10 mL) were added pyridine (1.50 mL, excess) and 10-undecenoyl chloride (0.66 g, 3.25 mmol). The resulting solution was continued with stirring at room temperature for 6 h. The desired product was isolated by washing with H_2O (30 mL \times 3) and brine (30 mL), dried over Na_2SO_4 , filtered, and concentrated to dryness. Flash column chromatography (hexane/

EtOAc = 15:1) afforded **5f** (0.13 g, 14%) as a white solid. ^1H NMR (CDCl_3 , 400 MHz): δ 8.70 (s, 1H), 5.88–5.73 (m, 2H), 5.02–4.90 (m, 4H), 2.59 (t, J = 3.6 Hz, 4H), 2.10–1.97 (m, 4H), 1.69–1.56 (m, 4H), 1.40–1.22 (m, 20H). ^{13}C NMR (CDCl_3 , 100 MHz): δ 174.6, 139.2, 114.2, 37.5, 33.8, 29.4, 29.3, 29.19, 29.17, 28.9, 24.4. HRMS (ESI): calcd for $\text{C}_{22}\text{H}_{40}\text{NO}_2$ 350.3059, found 350.3062 [$\text{M} + \text{H}$] $^+$.

5h. 10-Undecenoyl chloride (2.64 g, 13.0 mmol) in THF (10 mL) was added dropwise at 0 °C to a stirred solution of N,N' -dimethylethylenediamine (0.50 g, 5.67 mmol) and triethylamine (2.29 g, 22.6 mmol) in THF (15 mL). The mixture was stirred at this temperature for 2 h under argon atmosphere, after which it was allowed to warm to room temperature. After the mixture was stirred for another 6 h, THF was removed under reduced pressure. A saturated aqueous solution of NaHCO_3 (50 mL) was added, and the mixture was extracted with DCM (30 mL \times 3) and washed with brine (30 mL). The combined organic layer was dried over Na_2SO_4 , filtered, and concentrated to dryness. The residue was purified by flash column chromatography (hexane/EtOAc = 3:1) to afford **5h** (0.98 g, 41%) as a light yellowish liquid. ^1H NMR (CDCl_3 , 400 MHz): δ 5.84–5.74 (m, 2H), 4.99–4.89 (m, 4H), 3.50–3.43 (m, 4H, rotamer mixture), 3.01–2.94 (m, 6H, rotamer mixture), 2.31–2.21 (m, 4H, rotamer mixture), 2.04–1.99 (m, 4H), 1.62–1.55 (m, 4H), 1.40–1.22 (m, 20H). ^{13}C NMR (CDCl_3 , 100 MHz): δ 173.6, 173.5, 139.2, 114.2, 47.4, 47.0, 44.5, 37.1, 35.7, 33.8, 33.7, 33.6, 32.7, 29.59, 29.51, 29.45, 29.19, 28.98, 25.58, 25.09, 24.98. HRMS (ESI): calcd for $\text{C}_{26}\text{H}_{49}\text{N}_2\text{O}_2$ 421.3794, found 421.3789 [$\text{M} + \text{H}$] $^+$.

5i. 10-Undecenoyl chloride (2.25 g, 11.1 mmol) in DCM (10 mL) was added dropwise at 0 °C to a stirred solution of N -benzylethanolamine (0.8 g, 5.3 mmol) and triethylamine (2.1 g, 21.2 mmol) in DCM (30 mL). The mixture was stirred at this temperature for 2 h under argon atmosphere, after which time it was allowed to warm to room temperature. After being stirred for another 6 h, the reaction was quenched with H_2O (50 mL). The aqueous layer was extracted with DCM (30 mL \times 2), and the combined organic layers were washed successively with saturated aqueous solution of NaHCO_3 (30 mL \times 3) and brine (30 mL), dried over Na_2SO_4 , and concentrated to dryness. Flash column chromatography (hexane/EtOAc = 10:1 to 3:1) provided **5i** (1.50 g, 70%) as a light yellowish liquid. ^1H NMR (CD_2Cl_2 , 400 MHz): δ 7.28–7.06 (m, 5H), 5.78–5.70 (m, 2H), 4.94–4.80 (m, 4H), 4.53 and 4.52 (2s, 2H, rotamer mixture), 4.08 and 4.03 (2t, 2H, rotamer mixture), 3.49 (t, 1.1H, rotamer major), 3.41 (t, 0.9H, rotamer minor), 2.38–2.12 (m, 4H, rotamer mixture), 2.00–1.89 (m, 4H), 1.62–1.42 (m, 4H), 1.44–1.25 (m, 20H). ^{13}C NMR (CD_2Cl_2 , 100 MHz): δ 173.7, 173.3, 139.3, 138.0, 137.3, 128.8, 128.5, 127.6, 127.4, 127.1, 126.3, 113.8, 62.0, 61.4, 52.1, 48.3, 45.5, 45.0, 34.0, 33.8, 33.1, 33.0, 29.6, 29.5, 29.3, 29.2, 29.1, 28.9, 25.4, 25.3, 24.8. HRMS (ESI): calcd for $\text{C}_{31}\text{H}_{50}\text{NO}_3$ 484.3791, found 484.3791 [$\text{M} + \text{H}$] $^+$.

5l. 10-Undecenoyl chloride (2.68 g, 13.2 mmol) in DCM (10 mL) was added dropwise at 0 °C to a stirred solution of 1,5-pentanediol (0.59 g, 5.76 mmol) and pyridine (2.8 mL, 34 mmol) in DCM (15 mL). The mixture was stirred at this temperature for 2 h under argon atmosphere, after which it was allowed to warm to room temperature. After being stirred for another 6 h, the reaction was quenched with H_2O (50 mL). A standard extractive workup followed by flash column chromatography (hexane/EtOAc = 50:1) afforded **5l** (1.80 g, 71%) as a colorless liquid. ^1H NMR (CDCl_3 , 400 MHz): δ 5.83–5.73 (m, 2H), 4.98–4.88 (m, 4H), 4.04 (t, 4H, J = 6.8 Hz), 2.25 (t, 4H, J = 7.8 Hz), 2.03–1.98 (m, 4H), 1.67–1.55 (m, 8H), 1.43–1.26 (m, 22H). ^{13}C NMR (CDCl_3 , 100 MHz): δ 174.0, 139.2, 114.2, 64.0, 34.4, 33.8, 29.3, 29.28, 29.22, 29.1, 28.9, 28.3, 25.0, 22.5. HRMS (ESI): calcd for $\text{C}_{27}\text{H}_{49}\text{O}_4$ 437.3631, found 437.3622 [$\text{M} + \text{H}$] $^+$.

General Procedure for RCM Reaction. A diene substrate (0.50 mmol) and n -dodecane (0.25 mmol) were dissolved in dried and degassed dichloromethane (100 mL) to prepare a 5 mM substrate stock solution. An aliquot (10 mL) of this solution was added to catalyst (2.5 μmol , 5 mol % of substrate) in an oven-dried two-necked flask under a flow of argon to facilitate removal of ethylene. After being cooled to room temperature, the reaction progress was subjected to GC analysis. For the isolation of macrocyclic products **6a–l**, all

volatiles were removed under reduced pressure and the residue was purified by preparative thin-layer chromatography (PTLC). Isolated RCM products **6a**,^{2e} **6b**,^{2e} **6c**,¹⁹ and **6d**¹⁹ were identified by spectral comparison with literature reports.

6e. Hexane/EtOAc = 3:1 was used for PTLC. ^1H NMR (CDCl_3 , 400 MHz): δ 7.91 (d, 2H, J = 8.24 Hz), 7.33 (d, 2H, J = 8.24 Hz), 5.38–5.27 (m, 2H), 2.64 (t, 4H, J = 7.3 Hz), 2.45 (s, 3H), 2.08–1.92 (m, 4H), 1.72–1.61 (m, 4H), 1.39–1.27 (m, 20H). ^{13}C NMR (CDCl_3 , 100 MHz): δ 174.2, 145.4, 136.1, 130.4, 129.7, 128.9, 128.4, 39.2, 32.2, 29.7, 29.3, 29.1, 28.9, 27.9, 24.0, 21.8. HRMS (ESI): calcd for $\text{C}_{27}\text{H}_{42}\text{NO}_4$ 484.3791, found 484.3792 [$\text{M} + \text{H}$] $^+$.

6f. Hexane/EtOAc = 3:1 was used for PTLC. ^1H NMR (CD_2Cl_2 , 400 MHz): δ 8.28–8.18 (s, 1H), 5.41–5.30 (m, 2H), 2.60 (t, J = 6.4 Hz, 4H), 2.10–1.97 (m, 4H), 1.72–1.60 (m, 4H), 1.42–1.22 (m, 20H). ^{13}C NMR (CD_2Cl_2 , 100 MHz): δ 174.3, 130.6, 130.1, 37.3, 37.0, 32.1, 29.3, 29.2, 28.86, 28.82, 28.5, 28.4, 28.2, 27.8, 26.7, 24.9, 24.24. HRMS (ESI): calcd for $\text{C}_{20}\text{H}_{36}\text{NO}_2$ 322.2746, found 322.2745 [$\text{M} + \text{H}$] $^+$.

6g. Hexane/EtOAc = 10:1 was used for PTLC. ^1H NMR (CDCl_3 , 400 MHz): δ 5.35–5.27 (m, 2H), 4.27 (s, 4H), 4.23 (s, 4H), 2.28 (t, 4H, J = 7.3 Hz), 2.02–1.92 (m, 4H), 1.68–1.55 (m, 4H), 1.38–1.20 (m, 20H). ^{13}C NMR (CDCl_3 , 100 MHz): δ 173.6, 130.9, 130.1, 61.8, 34.5, 32.2, 29.39, 29.24, 29.14, 29.07, 29.00, 28.92, 28.23, 26.94, 25.35. HRMS (ESI): calcd for $\text{C}_{22}\text{H}_{39}\text{O}_4$ 367.2848, found 367.2856 [$\text{M} + \text{H}$] $^+$.

6h. Hexane/EtOAc = 1:2 was used for PTLC. ^1H NMR (CDCl_3 , 400 MHz): δ 5.36–5.23 (m, 2H), 3.58–3.43 (m, 4H, rotamer mixture), 2.98–2.91 (s, 6H, rotamer mixture), 2.28–2.18 (m, 4H, rotamer mixture), 2.06–1.94 (m, 4H), 1.61–1.45 (m, 4H), 1.35–1.15 (m, 20H). ^{13}C NMR (CDCl_3 , 100 MHz): δ 173.9, 173.8, 178.5, 173.3, 131.0, 130.6, 130.1, 129.9, 48.0, 46.9, 46.8, 43.6, 43.5, 37.7, 37.6, 35.2, 35.1, 33.9, 33.6, 33.0, 32.7, 32.2, 31.7, 30.1, 29.9, 29.8, 29.7, 29.4, 29.3, 29.2, 29.0, 28.9, 28.7, 28.5, 28.4, 28.2, 27.5, 26.8, 26.7, 26.4, 26.0, 25.8, 25.6, 25.0, 24.8. HRMS (ESI): calcd for $\text{C}_{24}\text{H}_{45}\text{N}_2\text{O}_2$ 393.3481, found 393.3488 [$\text{M} + \text{H}$] $^+$.

6i. Hexane/EtOAc = 3:1 was used for PTLC. ^1H NMR (CDCl_3 , 400 MHz): δ 7.38–7.12 (m, 5H), 5.39–5.27 (m, 2H), 4.62 and 4.58 (s, 2H, rotamer mixture), 4.24 (m, 1H, rotamer), 4.10 (m, 1H, rotamer), 3.64 (m, 1H, rotamer), 3.49 (m, 1H, rotamer), 2.50–2.29 (m, 4H, rotamer mixture), 2.08–1.92 (m, 4H), 1.75–1.58 (m, 4H), 1.42–1.21 (m, 20H). ^{13}C NMR (CD_2Cl_2 , 100 MHz): δ 174.3, 173.9, 173.8, 173.4, 137.4, 136.8, 130.9, 130.7, 129.0, 128.7, 128.0, 127.7, 127.5, 126.3, 61.1, 60.5, 51.4, 47.3, 45.2, 43.9, 34.6, 34.2, 33.6, 33.20, 33.23, 32.1, 32.0, 29.7, 29.6, 29.4, 29.3, 29.1, 29.0, 28.9, 28.8, 28.6, 28.3, 28.2, 27.8, 26.0, 25.9, 25.4, 25.0. HRMS (ESI): calcd for $\text{C}_{29}\text{H}_{46}\text{NO}_3$ 456.3478, found 456.3476 [$\text{M} + \text{H}$] $^+$.

6j. Hexane/EtOAc = 10:1 was used for PTLC. ^1H NMR (CDCl_3 , 400 MHz): δ 5.38–5.25 (m, 2H), 4.16 (td, 4H, J = 6.4, 1.8 Hz), 2.26 (td, 4H, J = 7.3, 1.8 Hz), 2.05–1.91 (m, 6H), 1.65–1.52 (m, 4H), 1.38–1.20 (m, 20H). ^{13}C NMR (CDCl_3 , 100 MHz): δ 173.9, 130.8, 130.1, 61.3, 61.1, 34.4, 32.1, 29.4, 29.2, 29.13, 29.10, 29.02, 29.0, 28.8, 28.7, 28.1, 27.8, 26.8, 25.1, 25.0. HRMS (ESI): calcd for $\text{C}_{23}\text{H}_{41}\text{O}_4$ 381.3005, found 381.3002 [$\text{M} + \text{H}$] $^+$.

6k. For the synthesis of **6k**, addition of 1,4-benzoquinone (10 mol % of substrate) was required to prevent olefin isomerization.^{14a} Hexane/EtOAc = 10:1 was used for PTLC. ^1H NMR (CDCl_3 , 400 MHz): δ 5.34–5.29 (m, 2H), 4.10 (t, 4H, J = 5.9 Hz), 2.30 (td, 4H, J = 7.3, 1.8 Hz), 2.06–1.91 (m, 4H), 1.75–1.55 (m, 8H), 1.38–1.20 (m, 20H). ^{13}C NMR (CDCl_3 , 100 MHz): δ 173.9, 130.7, 130.0, 63.8, 34.5, 32.3, 29.4, 29.1, 29.04, 28.99, 28.93, 28.2, 27.0, 25.5, 25.1. HRMS (ESI) calcd for $\text{C}_{24}\text{H}_{43}\text{O}_4$ 395.3161, found 395.3151 [$\text{M} + \text{H}$] $^+$.

6l. Hexane/EtOAc = 10:1 was used for PTLC. ^1H NMR (CDCl_3 , 400 MHz): δ 5.39–5.28 (m, 2H), 4.09 (t, 4H, J = 5.9 Hz), 2.29 (d, 4H, J = 7.7 Hz), 2.06–1.51 (m, 4H), 1.70–1.58 (m, 8H), 1.50–1.40 (m, 2H), 1.39–1.21 (m, 20H). ^{13}C NMR (CDCl_3 , 100 MHz): δ 174.0, 130.7, 130.1, 64.0, 34.5, 32.2, 29.4, 29.1, 29.0, 28.9, 28.7, 28.3, 28.25, 28.2, 26.9, 25.1, 22.9, 22.8. HRMS (ESI): calcd for $\text{C}_{25}\text{H}_{45}\text{O}_4$ 409.3318, found 409.3310 [$\text{M} + \text{H}$] $^+$.

■ ASSOCIATED CONTENT

■ Supporting Information

Characterization of the supported catalysts: BET, TEM image and EDS analysis, solid-state CPMAS ^{13}C and ^{29}Si NMR, ^1H and ^{13}C NMR spectra of all new compounds; GC traces for the *E,Z*-isomer of RCM products. This material is available free of charge via the Internet at <http://pubs.acs.org>.

■ AUTHOR INFORMATION

Corresponding Author

*E-mail: soonhong@snu.ac.kr, sslee@ibn.a-star.edu.sg.

Notes

The authors declare no competing financial interest.

■ ACKNOWLEDGMENTS

This research was supported by the Institute of Bioengineering and Nanotechnology (Biomedical Research Council, Agency for Science, Technology and Research, Singapore), the Research Center Program of IBS (Institute for Basic Science) in Korea, and the Basic Science Research Program through the National Research Foundation of Korea (NRF) funded by the Ministry of Education, Science and Technology (Grant No. 2012R1A1A1004077).

■ REFERENCES

- (1) (a) Han, S.-Y.; Chang, S. *Handbook of Metathesis*; Grubbs, R. H., Ed.; Wiley-VCH: Weinheim, 2003; Vol. 2, pp 5–127. (b) Fürstner, A. *Angew. Chem., Int. Ed.* **2000**, *39*, 3012–3043. (c) Nicolaou, K. C.; Bulger, P. G.; Sarlah, D. *Angew. Chem., Int. Ed.* **2005**, *44*, 4490–4527. (d) Rivkin, A.; Cho, Y. S.; Gabarda, A. E.; Yoshimura, F.; Danishefsky, S. J. *J. Nat. Prod.* **2004**, *67*, 139–143. (e) Khan, S. N.; Kim, A.; Grubbs, R. H.; Kwon, Y.-U. *Org. Lett.* **2011**, *13*, 1582–1585.
- (2) (a) Nolan, S. P.; Clavier, H. *Chem. Soc. Rev.* **2010**, *39*, 3305–3316. (b) Gradillas, A.; Perez-Castells, J. *Angew. Chem., Int. Ed.* **2006**, *45*, 6086–6101. (c) Monfette, S.; Fogg, D. E. *Chem. Rev.* **2009**, *109*, 3783–3816. (d) Conrad, J. C.; Eelman, M. D.; Silva, J. A. D.; Monfette, S.; Parnas, H. H.; Snelgrove, J. L.; Fogg, D. E. *J. Am. Chem. Soc.* **2007**, *129*, 1024–1025. (e) Fürstner, A.; Langemann, K. *Synthesis* **1997**, 792–803.
- (3) (a) Hong, S. H.; Wenzel, A. G.; Salguero, T. T.; Day, M. W.; Grubbs, R. H. *J. Am. Chem. Soc.* **2007**, *129*, 7961–7968. (b) Hong, S. H.; Day, M. W.; Grubbs, R. H. *J. Am. Chem. Soc.* **2004**, *126*, 7414–7415.
- (4) (a) Badjic, J. D.; Cantrill, S. J.; Grubbs, R. H.; Guidry, E. N.; Orenes, R.; Stoddart, J. F. *Angew. Chem., Int. Ed.* **2004**, *43*, 3273–3278. (b) Guidry, E. N.; Cantrill, S. J.; Stoddart, J. F.; Grubbs, R. H. *Org. Lett.* **2005**, *7*, 2129–2132. (c) Hou, H. Y.; Leung, K. C. F.; Lanari, D.; Nelson, A.; Stoddart, J. F.; Grubbs, R. H. *J. Am. Chem. Soc.* **2006**, *128*, 15358–15359. (d) Clark, P. G.; Guidry, E. N.; Chan, W. Y.; Steinmetz, W. E.; Grubbs, R. H. *J. Am. Chem. Soc.* **2010**, *132*, 3405–3412.
- (5) Halbach, T. S.; Mix, S.; Fischer, D.; Maechling, S.; Krause, J. O.; Sievers, C.; Blechert, S.; Nuyken, O.; Buchmeiser, M. R. *J. Org. Chem.* **2005**, *70*, 4687–4694.
- (6) (a) Schürer, S. C.; Gessler, S.; Buschmann, N.; Blechert, S. *Angew. Chem., Int. Ed.* **2000**, *39*, 3898–3901. (b) Mayr, M.; Buchmeiser, M. R.; Wurst, K. *Adv. Synth. Catal.* **2002**, *344*, 712–719. (c) Prühs, S.; Lehmann, C. W.; Fürstner, A. *Organometallics* **2004**, *23*, 280–287.
- (7) (a) Lim, J.; Lee, S. S.; Riduan, S. N.; Ying, J. Y. *Adv. Synth. Catal.* **2007**, *349*, 1066–1076. (b) Fischer, D.; Blechert, S. *Adv. Synth. Catal.* **2005**, *347*, 1329–1332. (c) Allen, D. P.; Wingerden, M. M. V.; Grubbs, R. H. *Org. Lett.* **2009**, *11*, 1261–1264.
- (8) (a) Vorfalt, T.; Wannowius, K.-J.; Plenio, H. *Agew. Chem., Int. Ed.* **2010**, *49*, 5533–5536. (b) Vorfalt, T.; Wannowius, K.-J.; Thiel, V.; Plenio, H. *Chem.—Eur. J.* **2010**, *16*, 12312–12315.
- (9) (a) Buchmeiser, M. R. *Chem. Rev.* **2009**, *109*, 303–321. (b) Hagiwara, H.; Nakamura, T.; Okunaka, N.; Hoshi, T.; Suzuki, T.

Helv. Chim. Acta **2010**, *93*, 175–182. (c) Coperet, C.; Basset, J. M. *Adv. Synth. Catal.* **2007**, *349*, 78–92. (d) Grela, K.; Tryznowski, M.; Bieniek, M. *Tetrahedron Lett.* **2002**, *43*, 9055–9059.

(10) (a) Lim, J.; Lee, S. S.; Ying, J. Y. *Chem. Commun.* **2008**, 4312–4314. (b) Lim, J.; Lee, S. S.; Ying, J. Y. *Chem. Commun.* **2010**, *46*, 806–808.

(11) (a) Macquarrie, D. H. *Ordered Porous Solids: Recent Advances and Prospects*; Valtechev, V., Mintova, S., Tsapatsis, M., Eds.; Elsevier: New York, 2008; p 725. (b) Molnar, A.; Rac, B. *Curr. Org. Chem.* **2006**, *10*, 1697–1726.

(12) (a) Kidder, M. K.; Britt, P. F.; Zhang, Z. T.; Dai, S.; Hagaman, E. W.; Chaffee, A. L.; Buchanan, A. C. *J. Am. Chem. Soc.* **2005**, *127*, 6353–6360. (b) Iwamoto, M.; Tanaka, Y.; Sawamura, N.; Namba, S. *J. Am. Chem. Soc.* **2003**, *125*, 13032–13033.

(13) Han, Y.; Lee, S. S.; Ying, J. Y. *Chem. Mater.* **2007**, *19*, 2292–2298.

(14) (a) Hong, S. H.; Sanders, D. P.; Lee, C. W.; Grubbs, R. H. *J. Am. Chem. Soc.* **2005**, *127*, 17160–17161. (b) Courchay, F. C.; Sworen, J. C.; Ghiviriga, I.; Abboud, K. A.; Wagener, K. B. *Organometallics* **2006**, *25*, 6074–6086.

(15) Absolute assignment of *E* and *Z* isomers was not facile. However, it has been suggested that the thermodynamically more stable *E* isomer is the major product as generally observed in olefin metathesis reactions. See ref 2e as well as characterization data and spectra for compounds **6a–I**.

(16) Hadinoto, S.; Lee, S. S.; Ying, J. Y. *Adv. Synth. Catal.* **2006**, *348*, 1248–1254.

(17) Weyl, H. *Synthesis of Peptides and Peptidomimetics*; Goodman, M., Felix, A., Moroder, L., Toniolo, C., Eds.; Georg Thieme Verlag Stuttgart: New York, 2002; Vol. 22, p 676.

(18) (a) Amoroso, D.; Yap, G. P. A.; Fogg, D. E. *Organometallics* **2002**, *21*, 3335–3343. (b) Amoroso, D.; Snelgrove, J. L.; Conrad, J. C.; Drouin, S. D.; Yap, G. P. A.; Fogg, D. E. *Adv. Synth. Catal.* **2002**, *344*, 757–763.

(19) Litinas, K. E.; Salteris, B. E. *J. Chem. Soc., Perkin Trans. 1* **1997**, 2869–2872.

(20) Warwel, S.; Tillack, J.; Demes, C.; Kunz, M. *Macromol. Chem. Phys.* **2001**, *202*, 1114–1121.

(21) Fokou, P. A.; Meier, M. A. R. *Macromol. Rapid Commun.* **2010**, *31*, 368–373.